Colloid Polym Sci (2007) 285:847-854
DOI 10.1007/s00396-006-1625-1

ORIGINAL CONTRIBUTION

Synthesis of monodisperse polymer microspheres by photopolymerization of microdroplets

Zhiqiang Gao · Eric A. Grulke · Asit K. Ray

Received: 15 August 2006 / Accepted: 19 November 2006 / Published online: 9 March 2007

Abstract We have examined photopolymerization of highly monodisperse microdroplets of monomer solutions under UV-light radiation. Microdroplets were generated using a modified vibrating aerosol generator, and the diameter of the droplets can be tuned to any size between 5 to 100 μm. Polymer particles derived from the droplets were characterized by optical microscopy and SEM. The results show that the polymer particles, under optimum conditions, can be highly spherical and monodisperse. The diameter and morphology of resulting microspheres depend on the diameter of the monomer solution droplets, monomer concentration, photopolymerization reaction temperature, residence time, and droplet dispersion.

Keywords Photopolymerization · Polymer microspheres · Vibrating orifice aerosol generator

Introduction

In recent years, polymer microspheres are finding ever increasing applications in various fields, such as drug delivery systems, biotechnology, optics, electronics and chemical technology. Several applications in emerging technologies, such as controlled release drug and optical microsensors, require highly monodisperse microspheres with very narrow size distributions. Polymer microspheres can be produced by a number of techniques. Emulsion based polymerization methods [1–7] can produce monodisperse particles with moderately narrow size distributions, but have some inherent drawbacks. The final product may include some undesirable components, such as surfactants or emulsifiers, and the size of the particles cannot be tuned arbitrarily. Polymer particles of various sizes have been prepared by contacting polymer solution droplets with an antisolvent that is completely miscible with the solvent for the polymer but immiscible with the polymer [8–10]. Use of dense gases (e.g., CO_2) as antisolvents yields particles that are free of residues. This technique, however, produces polydisperse particles of irregular shapes. The sedimentation polymerization technique [11–14], based on partial polymerization of individual monomer solution droplets as they settle through an immiscible liquid, has been successfully used to generate monodisperse spherical particles of size greater than 1 mm. Recently, Berkland et al. [15] have developed a technique based on the spraying of monodisperse polymer solution droplets into a solution where the droplets were solidified by extraction and evaporation. The monodisperse polymer solution droplets of controllable size were produced using a vibrating needle or an orifice through which the solution was pumped, and the size of the droplets controls the final size of microspheres. This technique can produce relatively monodisperse polymer microspheres ranging from a few to a few hundred micrometers. The disadvantage of the technique is that the droplets transform very slowly to solid particles in a liquid phase where they must be dispersed, and finally, centrifuged and dried to obtain solid particles.

Z. Gao · E. A. Grulke · A. K. Ray (✉)
Department of Chemical and Materials Engineering,
University of Kentucky, Lexington, KY 40506-0045, USA
e-mail: akray@engr.uky.edu

Among the solution based particle generation techniques precipitation polymerization is the most versatile method for producing nearly monodisperse surfactant-free spherical particles with narrow size distributions [16–23]. The particle size can be tuned from submicron to a few micrometers by controlling the initial composition of the reaction mixture and the polymerization conditions. The precipitation polymerization technique, however, has a number of limitations. The largest size of the particles obtainable through this method is about 5 μm. In addition, low monomer concentrations must be used to obtain monodisperse, unagglomerated particles, and only a fraction of the polymerized species transforms to solid particles. These factors result in a final product mixture that contains a dilute concentration of particles. As with other solution based methods, after polymerization particles must be separated by centrifugation or filtration, washed and then dried under vacuum.

Polymer particles can also be produced through aerosol based methods that involve transformation of monomer or polymer containing solution droplets to solid particles. These methods avoid the use of surfactants, and do not involve separation and drying of particles from liquid suspensions. The simplest aerosol based method is the spray drying technique, where droplets generated from a solution containing polymer dissolved in a volatile solvent are dispersed in a gas, and evaporation of solvent from the droplets leads to the formation of solid particles. The spray drying method usually produces particles with broad size distributions [24, 25], and the particles may not be spherical. Monodisperse solid particles of various morphologies have also been generated by reactions of droplets dispersed in a gas with coreactants [26–31].

The photo or radiation polymerization is one of the viable methods for manufacturing polymer microspheres. The radiation polymerization has been successfully used in liquid phase dispersions to produce microspheres [32, 33]. The studies [34–37] on photoinduced polymerization of single suspended monomer droplets have demonstrated that the photopolymerization technique can be applied to aerosol systems. Esen et al. [38, 39] were the first to show that monodisperse polymer microspheres can be produced by photopolymerization of monodisperse monomer solution droplets. In their method, monodisperse solution droplets produced by a vibrating aerosol generator were dispersed in a nitrogen atmosphere and allowed to evaporate. Finally, these droplets were transformed to solid spheres by photopolymerization induced by exposure to UV light. Their results show that monodisperse polymer microspheres of diameters ranging from 5 to 50 μm with a coefficient of variation (CV) of about 1% can be produced by the method.

In this paper, we examine photopolymerization of monodisperse monomer solution droplets, and the factors that control the morphology of the final polymer particles. Highly monodisperse droplets containing monomer dissolved in a volatile solvent were generated by a modified vibrating orifice aerosol generator. The polymerization reaction in the droplets was initiated by exposure to UV radiation. The droplet generator permits tuning of the droplet size to within 0.01% of the desired value in the size range 5–100 μm. The effects of the droplet size, monomer concentration, dispersion and reaction temperature on the final particles were examined.

Experimental

Materials

SOMOS 10220, commonly used in laser stereolithography for building three-dimensional parts, was purchased from DSM Desotech Inc., USA. It is a mixture of multiacrylate monomers 45–50%, epoxies 15–25%, polyols 20–35%, and photoinitiators 0.2–5%. As solvents for SOMOS 10220, we have used ethanol that was obtained from Aaper Alcohol and Chemical Co. All chemicals were used as is, without further purification.

Preparation of microspheres by photopolymerization

A schematic diagram of the experimental system used in this study is shown in Fig. 1. The system consists of a droplet generator, a cylindrical quartz reactor of 2.2 m length, irradiation sources and heating tapes. A solution of monomer (i.e., SOMOS 10220) dissolved in a highly volatile solvent (i.e., ethanol) was used to produce highly monodisperse droplets through a modified vibrating orifice aerosol generator (VOAG). The details of the VOAG and its operation can be found elsewhere [40–42]. Briefly, the solution in a reservoir is driven through a vibrating orifice under a constant gas pressure from a ballast tank, and the resulting cylindrical liquid jet passing through the orifice breaks into monodisperse droplets by the vibration of the orifice. The droplet diameter for a solution stream flowing at a volumetric rate of Q, through the orifice vibrating at a frequency f, is given by

$$D_d = \left(\frac{6Q}{\pi f}\right)^{1/3} \quad (1)$$

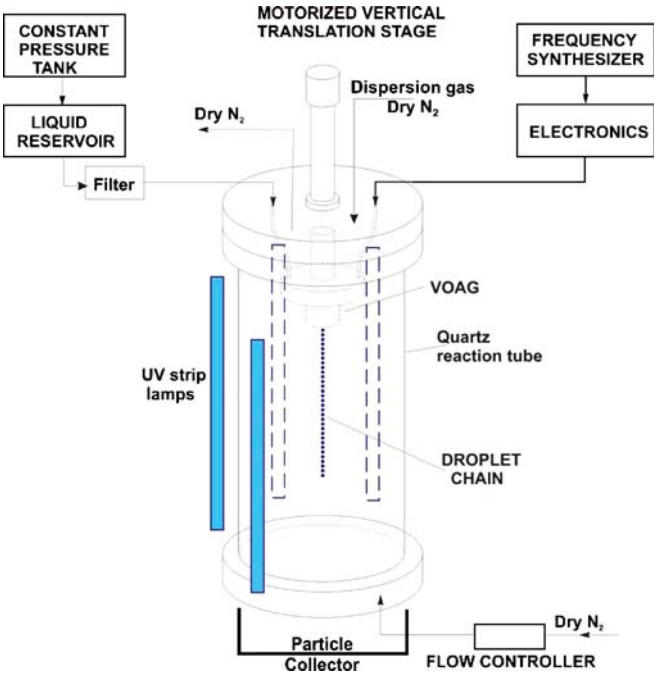

Fig. 1 Schematic of experimental system

The orifice is driven by a square wave with a frequency stability on the order of 1 part in 10^6, and the pressure difference driving the solution through the orifice is kept within 1 part in 10^5. The VOAG system is highly stable; we have shown that the short term fluctuation in the droplet size is about 1 part in 10^5, and the long term drift in the size is about of 0.01 nm/min [41]. Equation 1 shows that the droplet size depends on the solution flow rate and the frequency. The solution flow rate through the orifice depends on the gas pressure in the ballast tank and the orifice diameter, and for a given flow rate the droplets can be tuned in size over a range of about 20% by varying the orifice vibration frequency. Using an appropriate combination of the orifice diameter, the ballast tank gas pressure, and the orifice vibration frequency highly monodisperse droplets of any specific size can be produced in the diameter range 5–100 μm [40, 43].

Droplets for this study were generated from a solution of SOMOS 10220 dissolved in ethanol. The droplets were dispersed by nitrogen gas before introduction into the reaction chamber, and allowed to evaporate before exposure to UV radiation that is produced by eight 48″ long backlight fluorescent strip lamps. Each lamp provided 40 W of UV light at wavelength $\lambda = 355$ nm. To prolong the residence time of the droplets and to enhance solvent evaporation dry nitrogen gas was allowed to flow countercurrently past the droplets. The reaction chamber was heated to raise the activity of radicals and the monomer, and the temperature was controlled by heating tapes wrapped around the wall of the chamber. The particles emerging out of the reaction chamber were deposited on a collector.

Particle characterization

The collected particles were characterized by the optical microscopy and the scanning electron microscopy (SEM-Hitachi S-3200). The particles were examined under an optical microscope and sized with a calibrated staged micrometer. For SEM, the particles were placed on an aluminum sample holder and coated under vacuum with a thin layer of gold. More than 1,000 particles were measured and counted for the size distribution determination from each of the optical and SEM micrographs. The number mean diameter and the coefficient of variation were calculated from the size of the particles, and *ImageJ* program was used to determine the size of microspheres from their SEM images.

Results and discussion

We carried out photopolymerization experiments under various conditions. We varied the monomer solution flow rate through the orifice by varying the pressure in the ballast tank, the vibration frequency of the orifice, the orifice diameter, the monomer concentration and the reaction temperature. Table 1 lists the experimental parameters for five different experi-

Table 1 Summary of typical experimental conditions and results obtained from five separate experiments

Experiment #	1	2	3	4	5
Orifice dia. (μm)	15	20	15	20	15
Orifice frequency (kHz)	170	116	175	150	162
Dispersion gas flow rate (ml/s)	50	35	27	25	33
Reaction chamber temp. (°C)	65	60	60	91	55
Solution droplet dia., D_d (μm)	29.56	43.50	29.42	42.03	31.49
SOMOS vol. fraction, v_m	0.12	0.12	0.10	0.10	0.12
Mean residence time (s)	186	128	205	108	164
Polymer particle dia., $\bar{D}_p$ (μm)	14.7	21.9	13.8	-	16.0
Micrograph Fig. no.	2a	2b	3 & 4	5a & 5b	5c & 5d

ments. The solution flow rate and the frequency dictate the diameter of droplets as given by Eq. 1, and Table 1 includes droplet diameters calculated from Eq. 1. The optical micrographs of polymer particles produced from Experiment # 1 and Experiment # 2 are shown in Fig. 2a and b. The polymer particles resulting from the photopolymerization of monomer droplets in these experiments are spherical and monodisperse. Droplets in Experiment #2 were larger than Experiment # 1, but were generated from solutions containing the same concentration of monomer. Table 1 shows that the ratio of the diameters of the final polymer particles from these two experiments is nearly the same as the ratio of the initial diameters of the monomer solution droplets. Particles in Experiment # 3 were produced under the same experimental conditions as in Experiment #1, except for the monomer concentration. Use of the lower monomer concentration in the droplets of the former experiment results in the production of smaller size polymer particles. Figure 3 shows an optical micrograph of microspheres produced from Experiment #3 that were placed on a glass slide. The micrograph confirms that the microspheres are transparent as reflected by the presence of opalescence. Figure 4 shows SEM micrographs of particles prepared under the same experimental conditions. The sphericity and monodispersity of the polymer particles are evident in the micrographs. In addition, the enlarged micrograph of a particle in Fig. 4b shows that the surface of the particle is smooth. It should be noted that some of the particles in the micrograph in Fig. 4a appear as agglomerates, that is, two or more spherical particles adhering to each other during the solidification process. The percentage of agglomerates depends on the dispersion, and for dispersion gas flow rates used in these experiments we observed less than 5% agglomerates.

The size of microspheres is dictated by the size of the initial monomer solution droplets, the concentration of monomer, the solvent evaporation rate and the polymerization kinetics in the droplet. Another factor that plays an important role on the size and the morphology of the final solid particles is the reaction temperature. Higher temperatures lead to higher solvent evaporation rates as well as higher polymerization reaction rates. High temperature environments, however, cause rapid shrinkage of a droplet due to solvent evaporation, and at the same time rapid solidification of the region near the surface by photopolymerization induces structural stress in the particle that can result in the fracture of the particle. Figure 5a and b show examples of

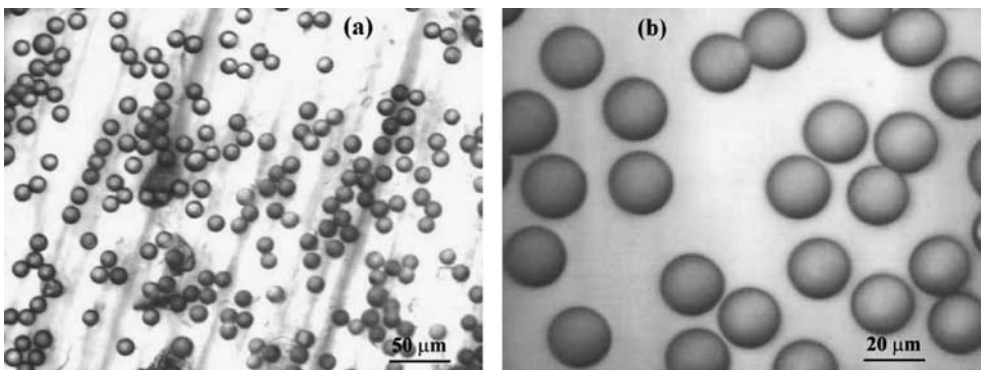

Fig. 2 Optical micrographs of polymer particles prepared by photo-polymerization. (**a**) particles produced under the conditions of Experiment # 1 listed in Table 1, (**b**) under the conditions of Experiment # 2 listed in Table 1

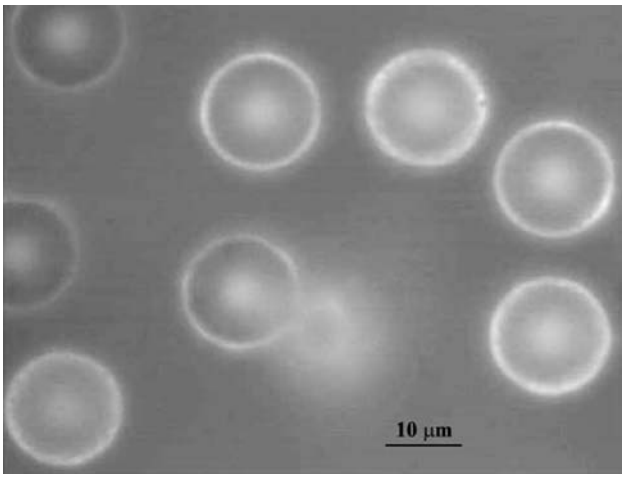

Fig. 3 Optical micrograph of polymer particles produced under the conditions of Experiment # 3 listed in Table 1. The particles were placed on a glass

fractured particles produced at a temperature of 91°C under conditions of Experiment # 4 in Table 1. Different complexities, however, arise at lower temperatures. Figure 5c and d show particles produced at 55°C under conditions of Experiment # 5 in Table 1. Slow polymerization produces a gooey surface through which solvent molecules escape nonuniformly, and as a result, ripple structures (i.e., golf-ball like) appear on the surface of the resultant particles. In addition, prolonged surface stickiness allows more particles to agglomerate as shown in Fig. 5c. There is a range of temperature, from about 60 to 90°, that yields microspheres with smooth surfaces as demonstrated by particles produced from Experiments #1 through #3.

For given experimental conditions the polymer microsphere size can be directly controlled through the size of the monomer solution droplets. As mentioned before, the monomer solution droplet size depends on the solution flow rate through the orifice and the orifice vibration frequency. The flow rate depends on the orifice diameter and the gas pressure in the ballast tank. For a given size orifice flow rate is proportional to the square root of the pressure drop driving the solution through the orifice. For a given flow rate the droplet size can be continuously tuned by varying the frequency. Figure 6 shows the effects of the orifice frequency and the pressure drop on the size of the polymer particles produced using a 20 μm orifice. For a given pressure drop (i.e., solution flow rate) the results show that the particle size decrease as the frequency increases, and is approximately proportional to $f^{-1/3}$, as expected from the relation for the monomer solution droplet diameter (i.e., Eq. 1). Furthermore, an increase in the pressure drop increases the diameter of the monomer solution droplets generated at a given frequency, and as a result, the polymer particle size versus frequency curve in Fig. 6 shifts upward as the pressure drop increases.

We have reported results in Table 1 and Fig. 6 on the basis of the mean polymer sphere diameter. We have examined more than 1,000 particles from each experiment to determine the size distribution, and the coefficient of variations in the diameters for our experiments were less than 1%. VOAG produces droplets whose diameters are contained within a coefficient variation of about 2×10^{-5}. We have shown that VOAG produced droplets, when traverse an identical path along the axis of the chamber, maintain the same monodispersity along the path, and the size and composition of the droplets are uniquely related to the position (i.e., distance traversed) [40–42].

Therefore, for given experimental conditions one expects the coefficient of variation in the size of the microspheres to be the same as that of the solution droplets. The results, however, show considerably higher variation in the microsphere size (i.e., $\sim$ 1%). This can be attributed, mainly, to the droplet dispersion used to prevent agglomeration among the particles. As a result of the dispersion, various droplets traversed various paths, and the residence times of the droplets varied slightly with the paths. In addition, the solvent evaporation rate was affected by the path (e.g., slower

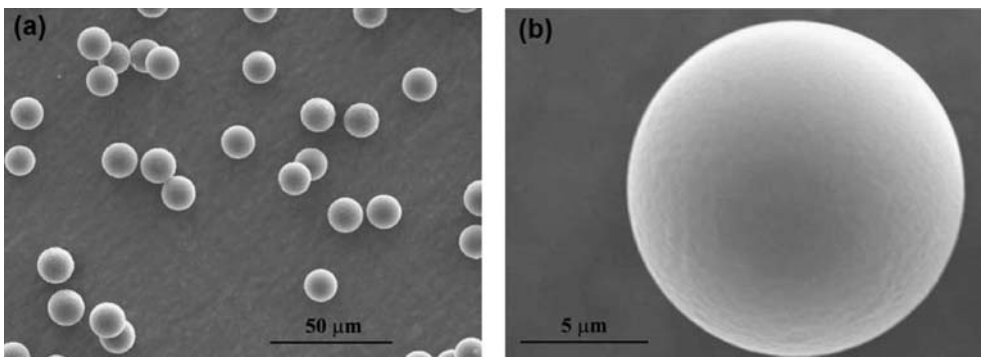

Fig. 4 SEM micrographs of polymer microspheres prepared under conditions of Experiment # 3 listed in Table 1. (**a**) particles with 600 times magnification, (**b**) particles with 6,000 times magnification

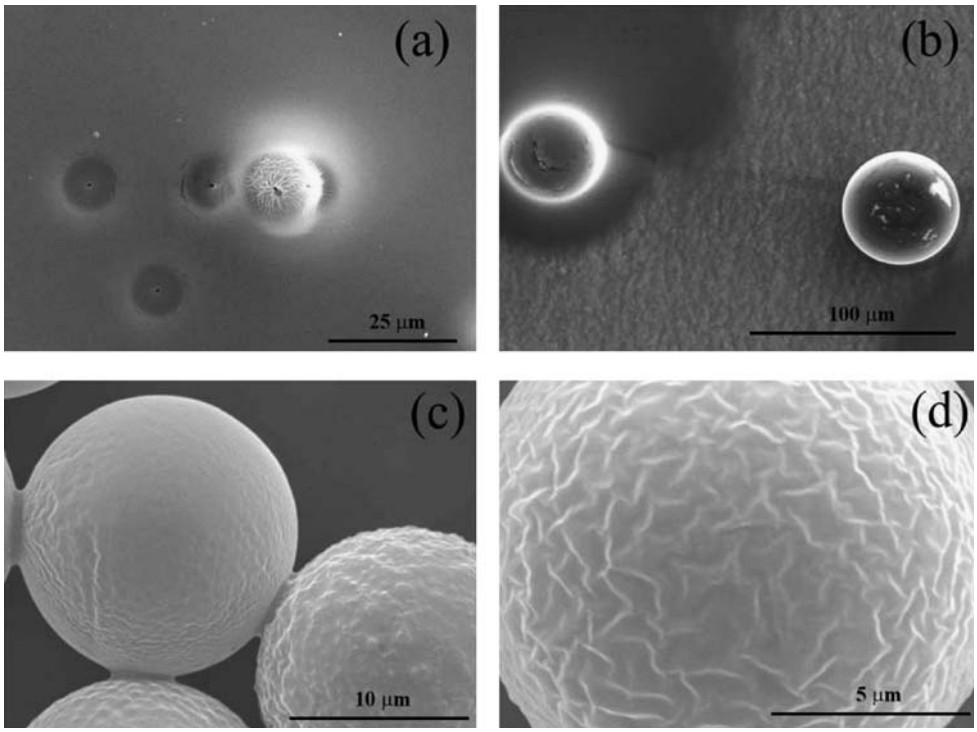

Fig. 5 SEM micrographs of polymer microspheres prepared at two different temperatures. (**a**) and (**b**) particles prepared under conditions of Experiment # 4 listed in Table 1, (**c**) and (**d**) particles from Experiment # 5 listed in Table 1

rate from the droplets near the chamber wall). The photopolymerization kinetics in a droplet was, in turn, influenced by the solvent evaporation, since the reaction rate depends on the monomer concentration and the particle structure.

Highly cross-linked macrostructures result from the photopolymerization of multifunctional monomers (e.g., tetraethyleneglycoldiacrylate and trimethylolpropane ethoxylate triacrylate) present SOMOS 10220. The photopolymerization increases density by converting double bonds to single bonds. As a result, the diameter of a polymer microsphere forming by photopolymerization of a solution droplet is expected to be smaller than the diameter of the particle that would result from the complete evaporation of the solvent without any polymerization, that is,

$$D_p < v_m^{1/3} D_d \tag{2}$$

where D_p is the diameter of the polymer microsphere resulting from the photopolymerization of a solution microdroplet of diameter D_d, containing monomer at a volume fraction v_m. The results in Table 1, however, show that the diameters of the microspheres in all the experiments are slightly (i.e., about 1–3%) higher than the solvent free monomer droplet diameter, $v_m^{1/3} D_d$. This suggests the microspheres produced in this study are porous. The porosity of a microsphere depends the degree of polymerization of the monomer molecules in a droplet. We have examined the effect of the reaction temperature on the apparent density (i.e., porosity) of microspheres. Figure 7 shows results from experiments where identical monomer solution droplets exposed to the reaction temperature that was varied from 50 to 90°C. Initially, the solution droplets were of 42.3 μm diameter, and contained 12 vol % monomer. The results show that the diameter of polymer microspheres decreases (i.e., apparent density in-

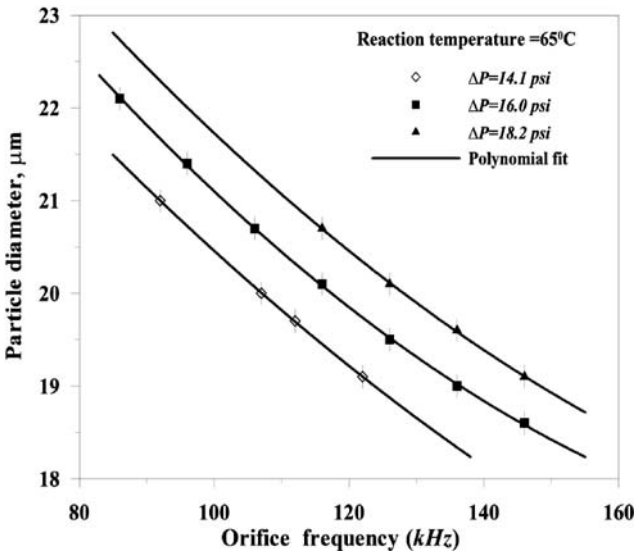

Fig. 6 Polymer microsphere size as a function of orifice vibration frequency for various pressure drops used to drive 12 vol % monomer solution through a 20 μm pinhole

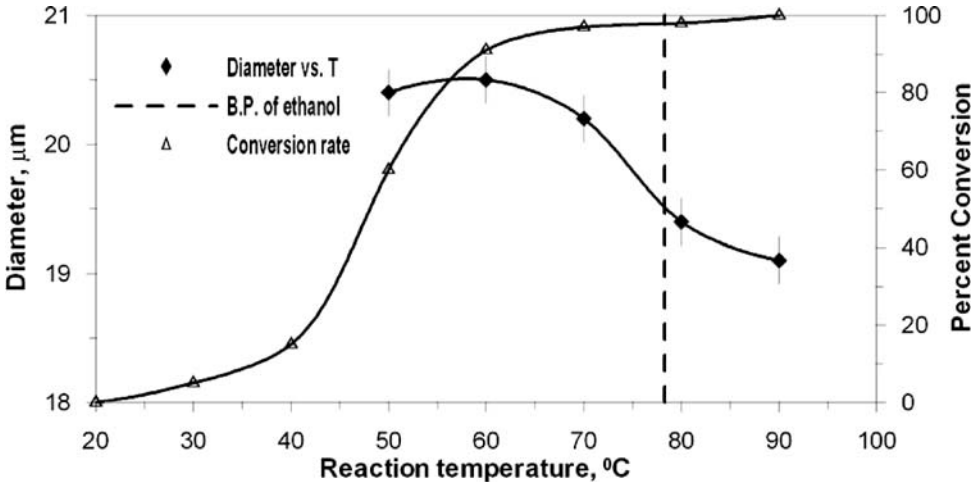

Fig. 7 Size of polymer microspheres prepared at various temperatures from identical solution droplets, and the results are compared with percent conversions of bulk samples by photopolymerization. Initially, the solution droplets were of 42.3 μm diameter, and contained 12 vol % monomer

creases) as the reaction temperature increases. The higher density results from the higher formation rate of macromolecules with cross-linked and network structures, as manifested by the bulk photopolymerization results shown in Fig. 6. The bulk experiments were conducted on monomer solution samples on transparent slides that were exposed to constant UV radiation for a period of 1 min. The percentage of conversion at a given temperature was determined from the polymer amount that remained undissolved after soaking the slide in ethanol. As expected, the results show that the fractional conversion over 1 min period increases slowly as the temperature increases from 20 to 40°C, then rises sharply till about 60°C, and finally, the polymerization reaction quenches as the conversion approaches 100% at around 90°C. The diameter of polymer microspheres qualitatively follows the results of bulk polymerization experiments, that is, the diameter decreases sharply between 60 and 80°C, but at much slower rates outside this temperature range. The temperatures shifted to higher values than the bulk because of the differences involved in the residence times and due to solvent evaporation.

Conclusions

We have presented a technique for generation of tailored microspheres of polymeric materials by in-situ photopolymerization of monomer solution droplets. Highly monodisperse droplets, with size fluctuations of less than 0.01%, were generated by a vibrating orifice aerosol generator (VOAG), and dispersed in air to prevent agglomeration. The droplets were photopolymerized by exposing them to ultra-violet light. The droplet size can be tuned to any desired value by controlling the volumetric flow rate of monomer solution through the orifice and the vibrating frequency of the orifice. A number of factors play critical role on the morphology of the final solid polymer particles. These factors include the monomer solution droplet diameter, the monomer concentration, the surrounding gas temperature, and dispersion. In this study we have demonstrated the aerosol based photopolymerization using a commercial monomer-photoinitiator mixture (i.e., SOMOS 10220). In principle, the technique of the present study can be used to generate polymer microspheres from any monomer with the use of an appropriate initiator that may exist in the droplet phase or in the vapor phase. For example, droplets of monomers of p-tertiary butylstyrene (TBS), styrene, and divinylbenzene (DVB) can be polymerized to microspheres using a vapor initiator, trifluo-romethanesulfonic acid (TFSA) [28, 29]. On the other hand acrylate monomer droplets can be photopolymerized using a droplet phase photoinitiator, Irgacure 369c [36]. One of the requirements, however, is that the polymerization kinetics must be fast enough to produce solid particles in short residence times involved in the reactor.

The results of our experiments suggest that tailored microspheres (e.g., multicomponent, layered, and with nanoparticle inclusions) of highly reproducible size and physical characteristics may be produced, and the morphology of the final solid polymer particles can controlled by the initial droplet size and composition as well as through the reaction conditions. We are currently investigating techniques for generation of such microspheres.

Acknowledgements The authors gratefully acknowledge the financial support of the National Science Foundation (grant # CTS-0130778), and the Kentucky Science & Engineering Foundation (grant # KSEF-456-RDE-005).

References

1. Tuin G, Peters ACI, Van Diemen AJG, Stein HN (1993) J Colloid Interface Sci 158(2):508
2. Keville KM, Franses EI, Caruthers JM (1991) J Colloid Interface Sci 144(1):103
3. Omi S (1996) Colloids Surf A., Physicochem Eng Asp 109:97
4. Ugelstad J, Mork PC, Kaggerud KH, Ellingsen T, Berge (1985) A Adv Colloid Interface Sci 13:101
5. Leroux J-C, Allémann E, Doelker E, Gurny R (1995) Eur J Pharm Biopharm 41:14
6. Arshady R (1991) J Control Release 17:1
7. Jonsson M, Nordin O, Malström E, Hammer C (2006) Polymer 47:3315
8. Young TJ, Johnston KP, Mishima K, Tanaka H (1999) J Pharm Sci 88:640
9. Reverchon E, Della Porta G (2001) Pure Appl Chem 73:1293
10. Tu LS, Dehghani F, Forster NR (2002) Powder Technol 126:134
11. Ruckenstein E, Hong L (1995) Polymer 36: 2857
12. Ruckenstein E, Sun Y (1996) J Appl Polym Sci 61:1949
13. Zhang H, Cooper AI (2002) Chem Mater 14:4017
14. Zhang H, Cooper AI (2005) Soft Matter 1:107
15. Berkland C, Kim K, Pack DW (2001) J Control Release 73:59
16. Li K, Stöver HDH (1993) J Polym Sci A Polym Chem 31: 3257
17. Li W-H, Stöver HDH (1998) J Polym Sci A Polym Chem 36: 1543
18. Li W-H, Stöver HDH (2004) Macromolecules 33:4354
19. Bai F, Yang X, Huang W (2004) Macromolecules 37:9746
20. Li S-H, Yang X-L, Huang W (2005) Chin J Polym Sci 37:9746
21. Bai F, Yang X, Li R, Huang B, Huang W (2006) Polymer 47:5775
22. Wang J, Cormack PAG, Sherrington DC, Khoshdel E (2003) Angew Chem Ind Ed 42:5336
23. Yang S, Shim SE, Choe S (2005) J Polym Sci A Polym Chem 43: 1309
24. Eerikäinen H, Kauppinen, EI, Kansikas (2004) J Pharm Res 21:136
25. Chu M, Zhou L, Song X, Pan M, Zhang L, Sun Y, Zhu J, Ding Z (2006) Nanotechnology 17:1791
26. Visca M, Matijević E (1979) J Colloid Interface Sci 68:308
27. Ingebrethsen BJ, Matijević E (1980) J Aerosol Sci 11:271
28. Partch RE, Matijevic E, Hodgson AW, Aiken BE (1983) J Polym Sci A 21:961-967.
29. Nakamura K, Partch R, Matijevic E (1984) J Colloid Interface Sci 99:118
30. Partch RE, Nakamura K, Wolfe EKJ, Matijevic E (1985) J Colloid Interface Sci 105: 560
31. Mayville FC, Partch RE, Matijević E (1987) J Colloid Interface Sci 120:135
32. Lee M-G (2002) Polymer 43:4307
33. Dai Q, Wu D, Zhang Z, Ye Q (2003) Polymer 44(1):73
34. Ward TL, Zhang SH, Allen T, Davis EJ (1987) J Colloid Interface Sci 118:343
35. Widmann JF, Davis EJ (1996) Colloid Polymer Sci 274(6):525
36. Widmann JF, Aardahl CL, Johnson TJ, Davis EJ (1998) J Colloid Interface Sci 199:197
37. Sprynchak V, Esen C, Schweiger G (2003) Aerosol Sci Technol 37:724
38. Esen C, Schweiger G (1996) J Colloid Interface Sci 179:276
39. Esen C, Kaiser T, Borchers MA, Schweiger G (1997) Colloid Polym Sci 275:131
40. Lin H-B, Eversole JD, Campillo AJ (1990) Rev Sci Instrum 61(3):1018
41. Devarkonda V, Ray AK, Kaiser T, Schweiger G (1998) Aerosol Sci Technol 28:531
42. Devarkonda V, Ray AK (2000) J Colloid Interface Sci 221:104
43. Berglun RN, Liu BYH (1973) Environ Sci Technol 7:147